2023 IEEE/ASME International Conference on Advanced Intelligent Mechatronics (AIM)
June 28-30, 2023. Seattle, Washington, USA

Dynamic Manipulation Like Normal-type Pen Spinning by a High-speed Robot Hand and a High-speed Vision System

Shoma Nakatani[1] and Yuji Yamakawa[2]

Abstract— This study presents a novel approach for dynamically manipulating an object, akin to standard pen spinning, by utilizing a high-speed robotic hand and visual feedback from a high-speed vision system. First, the dynamics of both standard pen spinning and the robotic hand are analyzed. Next, a pen spinning motion is developed for the robotic hand based on these dynamics. Experimental results of dynamic manipulation resembling conventional pen spinning demonstrate that the proposed simple motions of the robotic hand can achieve the desired dynamic (unstable) manipulation without the need for complex feedback controls.

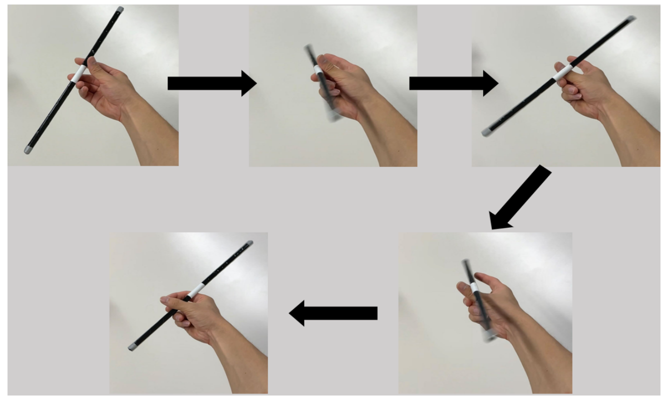

Fig. 1. Human pen spinning: Normal

I. INTRODUCTION

Research on multi-fingered robot hands capable of performing complex manipulations, akin to human hands, has made significant progress [1], [2]. However, it remains challenging to acquire the capability to execute complex and skilled object manipulations at high speeds, comparable to human abilities. To address this issue, dynamic manipulation has also been investigated [3]. One example of dynamic manipulation is dynamic regrasping, which involves changing the orientation of a grasped object. Previous studies have focused on regrasping cylindrical objects larger than a robot hand's fingers [4], as well as controlling the rotation of cylindrical objects smaller than a robot hand's fingers using pen spinning techniques [5], [6]. The former approach utilizes visual feedback to compensate for motion but does not aim to rotate the object. In contrast, the latter approach relies on feedback from touch sensors, ensuring the object remains in constant contact with the robot hand. Specifically, in the case of pen spinning, dynamic pen spinning has been achieved by rapidly rotating a pen on a finger, facilitated by high-speed motion and high-speed tactile sensory feedback.

In this study, we investigate pen spinning as an example of dynamic manipulation, specifically focusing on the ”normal type” of pen spinning. Normal type pen spinning, as typically performed by humans, is illustrated in Fig. 1, where the pen is flicked between the middle and thumb fingers, rotating around the thumb once and then caught. Previous research has explored scenarios where the manipulated object rotates slowly [4] or where pen spinning is performed while the object is stably held [5], [6]. The problem addressed in this study involves the robot hand undergoing an unstable state transition while spinning the pen for one full rotation, increasing the likelihood of the pen falling due to gravitational effects.

Previous work has also demonstrated the rotation of a flower stick using a robotic arm [7]. The flower stick is longer and heavier than a pen, resulting in a larger moment of inertia and more stable rotation. Additionally, the ”flowers” at both ends of the stick aid in decelerating the rotation. These characteristics make the flower stick easier to handle in rotational operations compared to a pen. Thus, this study aims to tackle more challenging dynamic manipulation tasks involving the manipulation of objects.

In the normal type pen spinning task, a more detailed dynamics analysis and vision-based feedback control for the robot are required compared to previous studies. This research aims to elucidate the dynamic skill [5], [6] involved in this operation, which involves the utilization of dynamic manipulation skills that capitalize on the interaction between the object and finger dynamics.

The pen spinning manipulation itself may lack practical utility beyond the act of pen spinning. However, the pen spinning motion serves as a demonstration of how the attitude of an object can rapidly change and appear complex, while its rapid manipulation can still be described and replicated in a relatively simple manner. Thus, research on pen spinning using a robotic hand can provide valuable insight towards efficient and low computational cost high-speed manipulation.

The proposed method utilizes a model of the pen and

[1]Shoma Nakatani is with School of Engineering, The University of Tokyo, 7-3-1 Hongo, Bunkyo-ku, Tokyo, Japan. nakatani-shoma251@g.ecc.u-tokyo.ac.jp

[2]Yuji Yamakawa is with Interfaculty Initiative in Information Studies, The University of Tokyo, 4-6-1 Komaba, Meguro-ku, Tokyo, Japan. y-ymkw@iis.u-tokyo.ac.jp

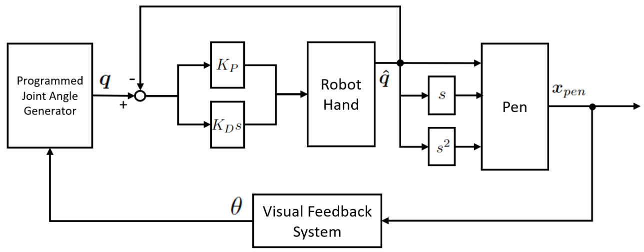

Fig. 2. Overall system of the normal type pen spinning task

robot hand, taking into account their respective dynamics, and determines the control variables for the robot hand to manipulate the pen using visual feedback. This process requires very fast movements. The contributions of this study are as follows:

- Generation of robot motion using the dynamics of the target object,
- Utilization of high-speed visual information for observation and feedback control, and
- Realization of stick-type dynamic manipulation with an unstable state.

II. ROBOT SYSTEM

Our system in this study consists of

- a high-speed robot hand shown in Fig. 3 (Section II-A),
- a high-speed vision system (Section II-B), and
- a real-time controller that receives the rotation angle of the pen from the image-processing PC at 1 kHz and also controls the high-speed robot hand at 1 kHz.

Fig. 2 shows the overall system for the normal pen spinning task, where the hand joint angles $\boldsymbol{q}$ at each time are determined by the program while referencing the pen's joint angle θ through the visual feedback system. The robot hand is controlled by PD control in response to this input $\boldsymbol{q}$, and the pen's posture is determined by the robot hand.

A. High-Speed Robot Hand

This high-speed robot hand [8], as shown in Fig. 3, consists of three fingers: right, middle, and left. The right and left fingers each have root and top joints and an additional joint at the root, enabling them to rotate towards the palm. In contrast, the middle finger only has root and top joints. Consequently, the degrees of freedom for these three fingers alone is 8, and when including the joints responsible for wrist rotation and those handling flexion and radial flexion, the total degrees of freedom for this robot hand is 10. The hand can change any joint angle by 180 degrees within 0.1 seconds. The reference joint angle can be set by a program, and the actual joint angle can be measured using an encoder. The joint angle can then be controlled using a PD (proportional and derivative) control law based on the difference between the reference and actual joint angles.

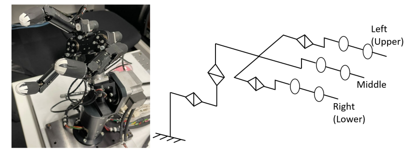

Fig. 3. High-speed robot hand

B. High-Speed Vision System

To measure the rotation angle of the pen, we used a high-speed vision system composed of a high-speed camera and an image-processing PC. The information on the rotation angle of the pen is used not only to confirm the validity of the proposed method but also to estimate the catching timing of the pen by the robot hand.

For the high-speed camera, we used a commercial high-speed camera, MQ013MG-ON, produced by XIMEA [10]. The image-processing PC was equipped with an Intel® Xeon® W5-1603 v3 2.8 GHz processor and 16 GB of RAM. The raw image data were 640 × 480 pixel, 8-bit grayscale images. After acquiring the image data every 2 ms, the image-processing PC calculates the coordinates of both ends of the pen within 2 ms and sends the computation results to the real-time controller via an Ethernet connection using the UDP protocol. The details of the image processing method are described in Section IV-A.

The camera was located on the front of the robot hand, which means that the optical axis of the camera is orthogonal to the rotation plane of the pen.

III. NORMAL-TYPE PEN SPINNING MOTION MODEL

A. Definition of Normal-type Pen Spinning

Pen spinning is a type of object manipulation that falls under the category of juggling, yo-yoing, and Kendama, among others. It is a form of performing art that involves using the fingers to manipulate an object. It is also one example of dynamic manipulation, which involves transitioning an object to a desired state through techniques such as pinching the pen with fingers, flicking it, and rotating it on one's hand or fingers. There are various techniques in pen spinning, and international competitions are held to compete in terms of the speed, number of rotations, and difficulty of these techniques. In the study by Namiki et al., dynamic manipulation was achieved through motions in which at least one finger of a robot hand is in contact with the object, referred to as the "drummer" and "sonic" types [5], [6].

In this study, we focus on normal-type pen spinning. As shown in Fig. 1, a typical normal-type pen spinning involves grasping the pen with the thumb, index, middle fingers, and ring finger, and then releasing the ring finger from the pen while pushing the center of mass or slightly above the center of mass with the middle finger, causing the pen to rotate approximately once so that the center of mass comes to the thumb.

However, the robot hand used in this study, as shown in Fig. 3, has only three fingers, which is fewer than the four required for a typical normal-type pen spinning. Additionally, the overall degree of freedom of the robot hand, which includes the two rotational joints of the wrist, is 10, which is less than the 12 degrees of freedom required for the three essential fingers (thumb, index, and middle fingers) in normal-type pen spinning manipulations performed by humans. Furthermore, the surface of the robot hand is not as smooth as a human hand. These physical constraints determine the conditions for achieving normal-type pen spinning with this robot hand.

B. Dynamics of Normal-type Pen Spinning Manipulation

In this context, a pen refers to a cylindrical pen-like object. By considering the dynamics of the pen and the hand, the necessary conditions for the hand motion can be determined to successfully perform the normal-type pen spinning manipulation. This compensates for the reproducibility and explainability of normal-type pen spinning and also leads to narrowing down the value of parameters in the hand movement program. In this case, the pen, or rod, is assumed to be non-deformable. A model of the hand seen from the direction of the rotation axis of the pen is shown in Fig. 4, with the pen represented relatively short. In this figure, the black circles represent the tips of hand fingers, which are referred to as upper finger, middle finger, and lower finger from top to bottom. Based on this model, the following topics are discussed in this paper:

(i) the initial attitude of the pen,
(ii) the initial relationship between the pen and the hand,
(iii) the position, velocity, and acceleration vectors of the tip of the middle finger,
(iv) the rotation motion of the pen, and
(v) the conditions for the pen not to fall when it is at Fig. 4(e).

Firstly, in (i), regarding the initial attitude of the pen, it is necessary to consider the required conditions for catching the pen regardless of its length (a longer pen has a wider catchable range). In normal pen spinning, the center of mass of the pen rotates approximately one rotation with each rotation of the thumb. After the pen is pushed by the upper and middle finger at the position shown in Fig. 4(a), the pen will depart from the hand at about 1/4 rotation, as shown in Fig. 4(b). To be able to catch the pen regardless of its length at this time, it is necessary for the gravity to act in the opposite direction to the velocity vector in a straight line. As a result, the initial posture of the pen should be parallel to gravity,

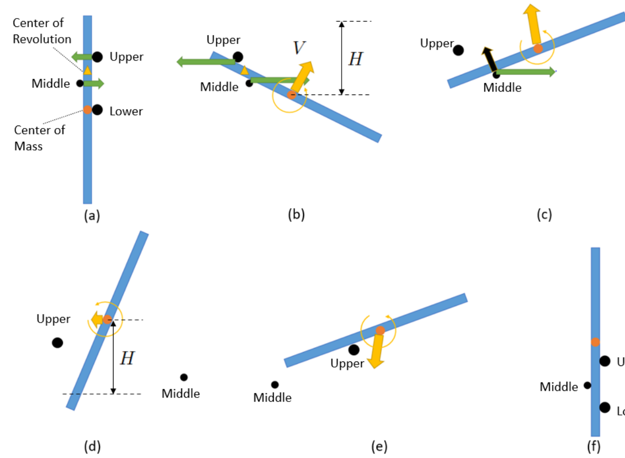

Fig. 4. Normal pen spinning model. The green arrow represents the vector of the hand finger tips' velocity, the thick yellow arrow represents the vector of the pen's center of mass velocity, and the thin yellow arrow represents the direction of the pen's rotation. The black arrow represents the vector of the force applied by the middle finger on the rod.

i.e., vertical to the horizontal plane, as shown in Fig. 4(a).

Secondly, in (ii), the relationship between the hand and the pen with mass m in their initial position is described. For the center of mass of the pen to rotate along with the upper finger in one rotation, the center of mass must at least surpass the height of the upper finger, as shown in Fig. 4(d) and (e). For example, let's assume the pen's center of mass rises by a height H from the position shown in Fig. 4(b), which is the moment when the hand can no longer exert force on the pen, and surpasses the height of the upper finger. To achieve this state, let the velocity of the pen's center of mass in the thick yellow arrow direction in Fig. 4(b) be V. If the distance between the center of mass and the rotation center is halved, the velocity will also be halved, resulting in $\frac{1}{2}m(\frac{V}{2})^2 \approx mg\frac{H}{4}$. Consequently, the required velocity of the center of mass to rise by a distance H beyond the upper finger is approximately four times V, and the angular velocity also becomes approximately four times necessary. However, this increases the speed of the pen in relation to the time resolution of the robot's movements and visual feedback, making it difficult to follow the movement of the pen. On the other hand, if the distance between the center of mass and the rotational center is increased, it leads to a greater lateral deviation in Fig. 4(c), making it difficult for the hand to catch the pen, depending on the attitude of the pen when the middle finger releases it.

Thirdly, in (iii) the position, velocity, and acceleration vector of the middle finger tip are described. The hand model is shown in Fig. 5, with each edge length given as AB $= L_{w0}$, BC $= L_{w1}$, CD $=$ CE $= L_p$, EF $= L_1$, FG $= L_2$. The length of the pen is L. In order for the hand to easily catch the pen, it is preferable for the

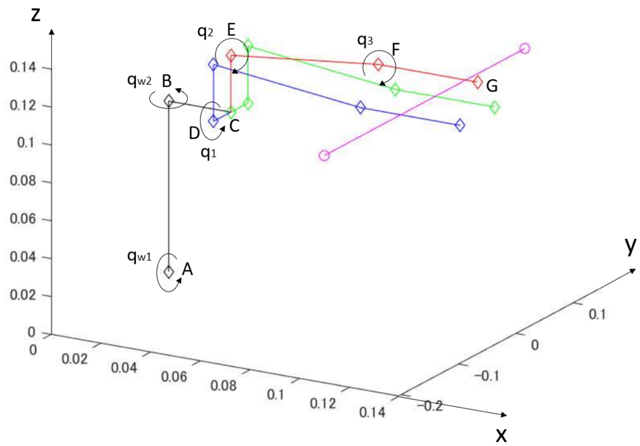

Fig. 5. Robot hand model

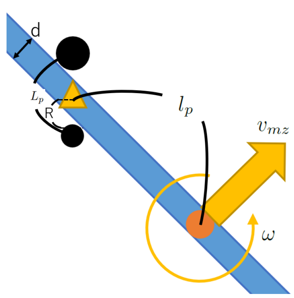

Fig. 6. Expanded view of contact point between the robot hand and the pen

pen's rotation axis to stay parallel to the x-axis without changing position. This condition is satisfied when $q_2 + q_3 = 0$. Assuming $q_{w1} = 0$ and $q_1 = 0$, the coordinate $\boldsymbol{x}_m$ of the middle finger tip of the hand is represented as follows.

$$\boldsymbol{x}_m = \begin{pmatrix} L_2 + L_1C_2 + L_{w1} \\ 0 \\ -L_1S_2 + L_r + L_{w0} \end{pmatrix}, \tag{1}$$

where q_1 is a joint angle of the top link, q_2 is a joint angle of the root link, and q_{w1} is a joint angle of the wrist joint. Also, C_i and S_i represent $\cos(q_i)$ and $\sin(q_i)$, respectively.

The velocity vector $\boldsymbol{x}_m$ and acceleration vector $\boldsymbol{a}_m$ of the middle finger tip are described based on the first and second derivatives of the finger tip coordinate $\boldsymbol{x}_m$.

$$\boldsymbol{v}_m = \dot{\boldsymbol{x}}_m \tag{2}$$

$$= \begin{pmatrix} -L_1S_2 \\ 0 \\ -L_1C_2 \end{pmatrix} \frac{dq_2}{dt} \tag{3}$$

$$\boldsymbol{a}_m = \dot{\boldsymbol{v}}_m \tag{4}$$

$$= \begin{pmatrix} -L_1C_2 \\ 0 \\ L_1S_2 \end{pmatrix} \left(\frac{dq_2}{dt}\right)^2 + \begin{pmatrix} -L_1S_2 \\ 0 \\ -L_1C_2 \end{pmatrix} \frac{d^2q_2}{dt^2} \tag{5}$$

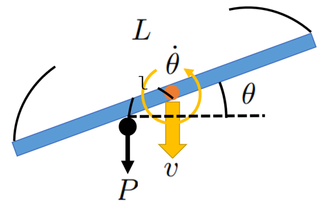

Fig. 7. Enlarged view of Fig. 4(e). For simplicity, the direction of the velocity vector of center of mass is assumed to be vertically downward.

Fourthly, in (iv) the rotational motion of a pen is described. In the motion of the pen rotating at an angular velocity ω with a point located at a distance l_p from its center as the rotational center, the motion is equivalent to the center rotating at angular velocity ω and the rod moving linearly in a direction perpendicular to it at a velocity of $l_p\omega$. In Fig. 6, when the upper and middle fingers are vertically aligned, the speed of their tips is denoted as v_{mz}, and the rotation radius is represented as R. Thus, $\omega = \frac{v_{mz}}{R}$.

Finally, in (v), the condition for the pen separate from the hand, rotate 1/2 turn, recontact the upper finger at the point shown in Fig. 4(e) and Fig. 7, and then complete another 1/4 rotation is described. In this case, the pen is not assumed to slip or detach from the finger. Let L be the length of the pen, and the direction of the velocity vector of the center of the pen immediately before and after the collision be v_0 and v, respectively. Also, let the angle between the pen and the horizontal plane at the time of the collision be θ, and the angular velocity before and after the collision be $\dot{\theta}_0$ and $\dot{\theta}$, respectively. Furthermore, let the downward-directed impulse force received by the pen be P, and the distance between the upper finger and the center of mass be l. The following conditions are satisfied.

$$mv_0 + P = mv \tag{6}$$

$$\frac{1}{12}mL^2\dot{\theta} = Pl\cos\theta + \frac{1}{12}mL^2\dot{\theta}_0 \tag{7}$$

$$v\cos\theta + l\dot{\theta} = 0 \tag{8}$$

The condition for the pen to remain in contact with the finger and rotate about 1/4 turn is represented by the following inequality.

$$\frac{1}{2}mv^2 + \frac{1}{2}\cdot\frac{1}{12}mL^2\dot{\theta}^2 > mgL(1-\sin\theta) \tag{9}$$

From Eqn. (6) to Eqn. (9), it is possible to estimate the conditions of the pen's angular velocity $\dot{\theta}_0(=\omega)$ before collision that allows the pen to rotate approximately 1/4 remaining.

IV. EXPERIMENTAL METHOD

A. Rotation Angle Measurement by a High-speed Image Processing Technique

In the visual feedback by high-speed camera, the timing of the robot hand catching the pen is derived by

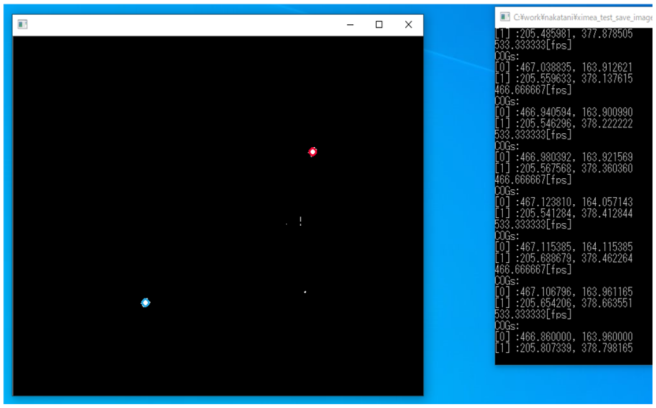

Fig. 8. Detection and calculation of tip coordinates by the visual feedback system

the angle of the pen calculated from the coordinate of its ends in camera image. The position of the ends of the pen are obtained using a target tracking algorithm [9]. A cylindrical object of a pen, with a diameter of 2.0 cm, a length of 35 cm, and a weight of 2 g made of styrene. By attaching recursive reflection tape wrapped around both ends of the pen and binarizing the captured image, the pen appeared white only at ends. The coordinates of the ends can be obtained by calculating the image centroid (x_g, y_g) of each retroreflective tape from their $(p+q)$-th order image moments $m_{p,q}$ as follows.

$$m_{p,q} = \sum_i \sum_j i^p j^q I(i,j), \tag{10}$$

$$x_g = \frac{m_{1,0}}{m_{0,0}}, \quad y_g = \frac{m_{0,1}}{m_{0,0}}, \tag{11}$$

where i and j are coordinates of horizontal and lateral directions in an image, and $I(i,j)$ is an intensity at (i,j) of the image.

By using the self-window method [9], once the reflection tape was captured and the centroid (x_g, y_g) was successfully calculated, a sub-frame region of interest (ROI) was set around the centroid. The ROI size was set to be smaller than the size of the original image to reduce the computational load. As a result, the coordinates of the both ends could be obtained at high speed as shown in Fig. 8. Then, we can obtain an rotation angle θ of the pen from the coordinates of the both ends. Their image processing and calculation could be performed every 2 ms.

B. Robot Hand Motion For Normal-type Pen Spinning

In Fig. 4(a)-(b), until the upper and middle fingers release the pen, the joint angles of the upper and middle fingers are symmetrical with respect to 0°, considering the axis passing through the midpoint of the tips of these two fingers as the axis of rotation of the pen. Under these conditions, the coordinates of the middle finger tip can be represented by Eqn. (1).

Fig. 6 shows an enlarged view of the location where the pen makes contact with the upper and middle fingers, as well as the vicinity of the center of mass of the pen when $q_2 = 0$, indicating that the upper and middle fingers are aligned in the y-axis direction. The two black circles represent the upper and middle fingers, respectively, with their radii denoted as r_u and r_m. The distance between the two fingers is denoted by L_p. The yellow triangle represents the rotational center, and the pen rotates around it with an angular velocity ω. The orange circle represents the center of mass, which is moving in the z-axis direction with velocity v_{mz}. The distance between the rotational center and the center of mass is denoted as l_p. Let d represent the diameter of the pen, and let $t = t_1$ represent the time at this moment. The rotation radius R, the velocity of the center of mass in the z-axis direction v_{mz}, and the angular velocity ω can be represented as functions of constraints and the middle finger root joint angle q_2, as follows.

$$R = \frac{1}{2}\left\{L_p - \frac{d + r_u + r_m}{L_p}(r_u + r_m)\right\} \tag{12}$$

$$v_{mz} = L_1 \cos(0) \left.\frac{dq_2}{dt}\right|_{t=t_1} = L_1 \left.\frac{dq_2}{dt}\right|_{t=t_1} \tag{13}$$

$$\omega = \frac{v_{mz}}{R} \tag{14}$$

Next, the necessary conditions for the middle finger root joint velocity at $t = t_1$ to grasp the pen after releasing it is determined. Let $l = xL$, from Eqn. (6) to Eqn. (9) and $v_0 = l_p\dot{\theta}_0$, the following inequality is obtained.

$$\frac{1 - 12 l_p x \cos\theta}{1 + 12x^2}\dot{\theta}_0 > \frac{2gx(1 - \sin\theta)}{L\left(\frac{x^2}{\cos\theta} + \frac{1}{12}\right)} \tag{15}$$

For simplicity, let $\theta = 0$, from Eqn. (12) to Eqn. (14), the necessary conditions for the middle finger root joint velocity can be represented by only one variable x as follows.

$$\left.\frac{dq_2}{dt}\right|_{t=t_1} > \frac{24gx\left\{L_p - \frac{d+r_u+r_m}{L_p}(r_u + r_m)\right\}}{LL_1(1 - 12 l_p x)} \tag{16}$$

Additionally, let q_2 be represented as follows.

$$q_2 = at^2 + bt + c \tag{17}$$

If $a = 0$, it follows from Eqn. (5) that the second term is $\mathbf{0}$ when $q_2 = 0$ $(t = t_1)$ and the z-component of the first term is also 0. This indicates that the couple of force exerted by upper and middle finger to the pen is 0 when $q_2 = 0$. At this time, referring to Eqn. (3), the velocity in the x-axis direction is 0. However, releasing the pen when $q_2 = 0$, that is, releasing the pen at the most fingertip side, means that the hand cannot control the pen if it rolls even slightly in the positive x-axis direction. Thus, $a \neq 0$, by adjusting the values of a, b, and c at an arbitrary location to some extent, the couple of force against the pen can be set to 0, making it possible to release the pen. Furthermore, by adjusting the value of x, it is possible to determine where the upper finger collides with the pen, as shown in Fig. 4(e) and Fig. 7.

In Fig. 4(e)–(f), the angle of the pen is calculated from the coordinates of both ends of the pen obtained using a high-speed camera, and the hand transitions to a position to catch the pen based on that angle.

The other finger motions change from the initial position to the catching position while avoiding interference with the spinning pen.

V. EXPERIMENTAL RESULT

The results of the normal-type pen spinning using the high-speed robot system are shown in Fig. 9, and the time-varying change of the pen's angle, obtained from the coordinates of both ends of the pen, is shown in Fig. 10. The normal-type pen spinning task performed by the robot hand took approximately 0.42 seconds. The video of the experimental results can be viewed on the website [11].

Fig. 9(I)–(VI) correspond approximately to Fig. 4(a)–(f). Fig. 9(I) shows the initial state, with the lower finger positioned approximately at the pen's center of mass. In Fig. 9(II), the moment when the upper finger separates from the pen is captured. The pen does not touch the upper finger from Fig. 9(II) to (V). In Fig. 9(III), the moment when the middle finger leaves the pen is shown. If the middle finger released the pen later, the pen would rise higher to the left. Conversely, if the middle finger released the pen earlier, the pen would rise higher to the right. In Fig. 9(III), the timing of the middle finger's release from the pen is appropriate, resulting in the pen moving upward and slightly to the left from directly above, with its center of mass higher than the upper finger, as seen in Fig. 9(IV). At this point, the upper finger has adjusted its position to grasp the pen. In Fig. 9(V), the collision between the upper finger and the pen occurs. This is evident in Fig. 10, where the slope of the graph changes before and after Fig. 9(V), indicating that the pen collided with the upper finger at this point. The use of visual feedback system was motivated by the need to address the change in the pen's rotation speed caused by the collision between the upper finger and the pen. By utilizing visual feedback system, the angle of the pen could be monitored and used to determine the timing for the robot hand to grasp the pen. In the end, as shown in Fig. 9(VI), the robot hand successfully catches the pen. After Fig. 9(VI), as shown in Fig. 10, the angle of the pen changes slightly due to the pen bending and vibrating when the hand catches it.

Fig. 11 shows the graph of the programmed angle and the actual angle of the root joint of the middle finger, which is particularly important in normal-type pen spinning manipulation, as a function of time. The actual joint angle values deviated from the programmed values between Figs. 9(III) and (IV), and in some parts between Figs. 9(IV) and (VI), because the robot hand

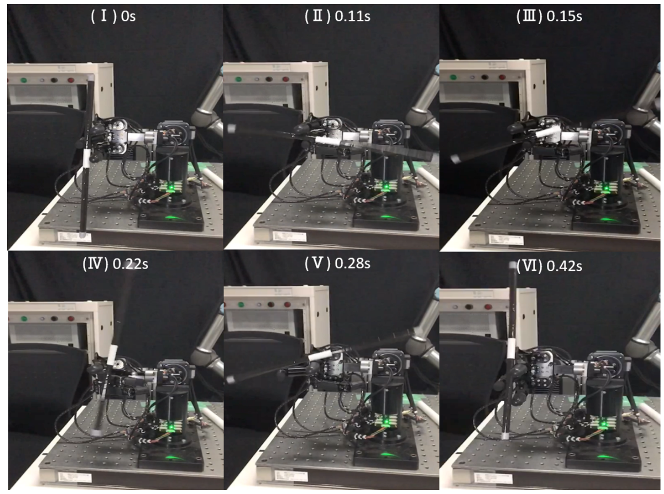

Fig. 9. Result of normal pen spinning. These images were extracted as still frames from slow-motion videos taken with an iPhone 6S.

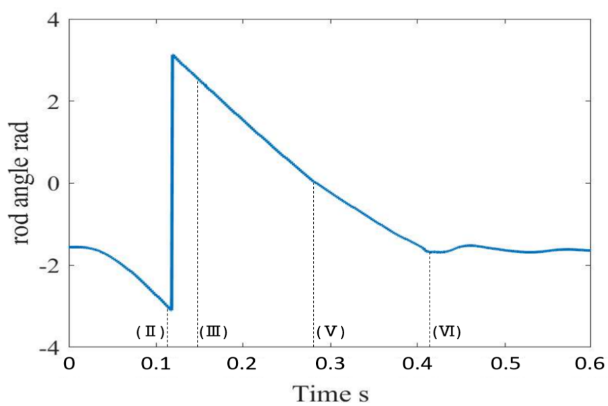

Fig. 10. Result of rotation angle of pen

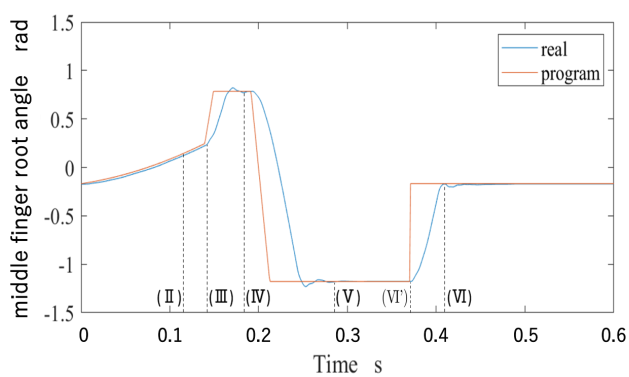

Fig. 11. Joint angle of root link of middle finger

used in the experiment was capable of changing the angle by 180 degrees in 0.1 seconds, but was given instruction values exceeding that. As described in Section IV-B, until Fig. 9(Ⅱ), the tip joint angle and the root joint angle of the middle finger were symmetrical to 0 degrees, and furthermore, the joint angles of the middle finger were symmetrical to 0 degrees in comparison to those of the upper finger. Both the value of the programmed and actual root angle were determined by a second-order function with respect to time until Fig. 9(Ⅱ), and by a linear function with respect to time until Fig. 9(Ⅲ). By doing this, the pen was no longer subject to a couple of forces exerted by the upper and middle fingers at Fig. 9(Ⅱ), and the pen separated from the upper finger, as shown in Fig. 9. On the other hand, the pen remained on the middle finger due to gravity and the slow speed of the middle finger tip compared to the rotation speed of the pen. Therefore, in Fig. 9(Ⅲ), it was possible to release the pen from the middle finger by rapidly changing the joint angle. The motion of the middle finger from Fig. 9(Ⅲ) to (V) was intended to change the attitude of the middle finger from the position where it released the pen to the position before catching the pen without any interference from the pen. Based on the information of the rotation angle of the pen in Fig. 10, the timing of starting to catch the pen in Fig. 9(Ⅵ') was obtained, and the middle finger transitioned to the attitude for catching the pen from Fig. 9(Ⅵ') to (Ⅵ).

VI. CONCLUSION

The normal-type pen spinning task was performed in less than 0.5 seconds, and there existed a state where the object, which was to rotate once, could not be controlled stably. However, by considering the dynamics of the pen and the hand and focusing on the motion of separating the pen from the hand, it was possible to control the robot hand with low computational cost and achieve normal-type pen spinning manipulation. Additionally, this study demonstrates that the control of the robot hand can efficiently control the rotational motion of an object by applying force to it for only a moment.

One of the future research tasks is to perform multiple rotations of a pen. The methods developed in this study can be applied to multiple rotations of a pen while it is floating away from the robot hand. However, for multiple rotations while the pen is in contact with the hand, the robot hand should ideally have at least three degrees of freedom, similar to a human thumb, to face the other fingers. To achieve this, a smooth-surfaced finger that can enable the pen to rotate around its center of mass must be developed. Additionally, a control system that recognizes the center of mass of the pen through visual feedback, and minimizes linear motion of the pen as much as possible, is also necessary.

References

[1] A. Bicchi: Hands for dexterous manipulation and robust grasping: A difficult road toward simplicity, IEEE Trans. Robot. and Automat., Vol.16, No.6, pp.652–662, 2000.

[2] A. Saudabayev and H. A. Varol: Sensors for Robotic Hands: A Survey of State of the Art, IEEE Access, Vol.3, pp.1765–1782, 2015.

[3] M. T. Mason and K. M. Lynch: Dynamic Manipulation, Proc. IEEE/RSJ Int. Conf. Intelligent Robots and Systems, pp.152–159, 1993.

[4] N. Furukawa, A. Namiki, T. Senoo, and M. Ishikawa: Dynamic regrasping using a high-speed multifingered hand and a high-speed vision system, Proc. IEEE Int. Conf. on Robotics and Automation, pp.181–187, 2006.

[5] T. Ishihara, A. Namiki, M. Ishikawa, and M. Shimojo: Dynamic Pen Spinning Using a High-speed Multifingered Hand with High-speed Tactile Sensor, Proc. 2006 IEEE RAS Int. Conf. on Humanoid Robots, pp.258–263, 2006.

[6] A. Namiki, T. Ishihara, Y. Yamakawa, M. Ishikawa and M. Shimojo: Rotational Control of A Stick Using a High-speed Multifingered Hand, Proc. 13th Robotics Symposia, pp.541–546, 2007. in Japanese

[7] T. Aoyama, T. Takaki, T. Miura and I. Ishii: Rotating Manipulation of Flower Stick Based on Only Consideration of Kinematic Constraint, Journal of the Robotics Society of Japan, Vol.35, No.3, pp.258–266, 2017. in Japanese

[8] A. Namiki, Y. Imai, M. Ishikawa, and M. Kaneko: Development of a high-speed multifingered hand system and its application to catching, Proc. IEEE/RSJ Int. Conf. on Intelligent Robots and Systems, pp.2666–2671, 2003.

[9] I. Ishii and M. Ishikawa: Self Windowing for High Speed Vision, Proc. IEEE Int. Conf. Robotics and Automation, pp.1916-1921, 1999.

[10] XIMEA. Available online: https://www.ximea.com/ (accessed on 9 February 2023).

[11] Yamakawa Lab. Available online: http://www.hfr.iis.u-tokyo.ac.jp/research/PenSpinning/AIM2023.mp4 (accessed on 9 February 2023).